THE JOURNAL OF BIOLOGICAL CHEMISTRY VOL. 286, NO. 1, pp. 270–279, January 7, 2011

Interaction of *Escherichia coli* RNA Polymerase σ^{70} Subunit with Promoter Elements in the Context of Free σ^{70}, RNA Polymerase Holoenzyme, and the β'-σ^{70} Complex*[S]

Received for publication, August 11, 2010, and in revised form, September 23, 2010 Published, JBC Papers in Press, October 15, 2010, DOI 10.1074/jbc.M110.174102

Vladimir Mekler[‡1], **Olga Pavlova**[‡], **and Konstantin Severinov**[‡§2]

From the [‡]*Waksman Institute of Microbiology, Rutgers, State University of New Jersey, Piscataway, New Jersey 08854 and the* [§]*Institutes of Molecular Genetics and Gene Biology, Russian Academy of Sciences, 119334 Moscow, Russia*

Promoter recognition by RNA polymerase is a key point in gene expression and a target of regulation. Bacterial RNA polymerase binds promoters in the form of the holoenzyme, with the σ specificity subunit being primarily responsible for promoter recognition. Free σ, however, does not recognize promoter DNA, and it has been proposed that the intrinsic DNA binding ability is masked in free σ but becomes unmasked in the holoenzyme. Here, we use a newly developed fluorescent assay to quantitatively study the interactions of free σ^{70} from *Escherichia coli*, the β'-σ complex, and the σ^{70} RNA polymerase (RNAP) holoenzyme with non-template strand of the open promoter complex transcription bubble in the context of model non-template oligonucleotides and fork junction templates. We show that σ^{70}, free or in the context of the holoenzyme, recognizes the −10 promoter element with the same efficiency and specificity. The result implies that there is no need to invoke a conformational change in σ for recognition of the −10 element in the single-stranded form. In the holoenzyme, weak but specific interactions of σ are increased by contacts with DNA downstream of the −10 element. We further show that region 1 of σ^{70} is required for stronger interaction with non-template oligonucleotides in the holoenzyme but not in free σ. Finally, we show that binding of the β' RNAP subunit is sufficient to allow specific recognition of the TG motif of the extended −10 promoter element by σ^{70}. The new fluorescent assay, which we call a protein beacon assay, will be instrumental in quantitative dissection of fine details of RNAP interactions with promoters.

Bacterial RNA polymerase (RNAP)[3] initiates transcription in the form of the holoenzyme (subunit composition $\alpha_2\beta\beta'\omega\sigma$). The RNAP core enzyme ($\alpha_2\beta\beta'\omega$) is catalytically competent but does not recognize promoters. Available biochemical, structural, and genetic data clearly show that, within the holoenzyme, σ is responsible for the recognition of promoter consensus elements located, at most promoters, ~10 and ~35 bp upstream of the transcription start site (located at +1) (1–3). Although some promoters lack the −35 element (and hence do not require σ region 4 for promoter complex formation), the −10 promoter element is strictly required. However, the −10 promoter element on its own is not sufficient for promoter complex formation. In the absence of the −35 element, additional elements such as a TG*X* motif upstream of the −10 element or downstream GGGA motif are required for efficient promoter recognition (4, 5).

The −10 promoter element is recognized by σ region 2. Although original recognition must proceed in the form of double-stranded DNA, in transcription-competent open complex, the −10 element is present in single-stranded form as part of the transcription bubble, which on most promoters extends from −12 to approximately +3. Although open complex formation by RNAPs from mesophilic organisms such as *Escherichia coli* takes place under conditions at which the double-stranded form of DNA is resistant to denaturation by about 1 kcal/mol bp, many open complexes are very stable (6). Because of high energetic cost of transcription bubble formation, the RNAP-promoter interactions responsible for this process must be very strong. An important source of energy driving the strand separation process and controlling the open complex stability is the interaction of RNAP with the non-template strand of the transcription bubble (6–8).

In the open complex, σ region 2 makes specific contacts with the non-template strand of the −10 promoter element (consensus sequence TATAAT for *E. coli* σ^{70} as well as for housekeeping σ factors of many other bacteria). Adenine at position −11 of the non-template strand is of special importance for nucleation of promoter melting (9). Outside of the −10 element, a non-template segment of the transcription bubble corresponding to positions −6 to −3 interacts with σ region 1.2 (10) and cross-links to the RNAP β subunit (11). Further downstream, a non-template segment of the transcription bubble surrounding the transcription start point (positions −2 to +2) interacts with β (11). Gralla and coworkers (12) showed that inclusion of the non-template segment corresponding to positions −6 to +1 stimulates the binding of fork junction probes, which consist of double-stranded upstream promoter DNA with single-stranded se-

* This work was supported, in whole or in part, by National Institutes of Health Grant R01 GM64530 (to K. S.). This work was also supported by a Charles and Johanna Busch postdoctoral fellowship (to O. P.) and Russian Academy of Sciences Presidium Program in Molecular and Cellular Biology (to K. S.).

[S] The on-line version of this article (available at http://www.jbc.org) contains supplemental Figs. S1–S3 and Table S1.

[1] To whom correspondence may be addressed: Waksman Institute, Rutgers, State University of New Jersey, 190 Frelinghuysen Rd., Piscataway, NJ 08854. Tel.: 732-445-6096; Fax: 732-445-5735; E-mail: mekler@waksman.rutgers.edu.

[2] To whom correspondence may be addressed: Waksman Institute, Rutgers, State University of New Jersey, 190 Frelinghuysen Rd., Piscataway, NJ 08854. Tel.: 732-445-6096; Fax: 732-445-5735; E-mail: severik@waksman.rutgers.edu.

[3] The abbreviations used are: RNAP, RNA polymerase; oligo, oligonucleotide; TMR, tetramethylrhodamine-5-maleimide; PET, photoinduced electron transfer.

quences downstream of positions −11 or −12. It is unknown, however, whether such increased binding is sufficient to mediate formation of the transcription bubble.

Specific interaction of oligonucleotides mimicking the non-template strand of the transcription bubble in the open promoter complex (*i.e.* containing the −10 promoter element and downstream DNA up to position +1) with σ is readily detected using biochemical methods such as protein-DNA cross-linking or native gel electrophoresis in the context of the holoenzyme (8). In fact, isolated β' or a β' fragment containing the primary σ-binding site is sufficient to allow relatively strong interaction between σ (or σ fragment containing region 2) with such oligonucleotides (13, 14). These results were interpreted as suggesting that, upon formation of the holoenzyme, the intrinsic −10 element binding capacity of σ is either unmasked (by removing an inhibitory interaction that is present in free σ and that prevents promoter recognition) or increased (by introducing a conformational change and/or readjusting the DNA binding domain of σ). Indeed, it is now well established that σ does undergo large scale conformational changes upon holoenzyme formation that affect the relative positions of its DNA binding domains (15, 16).

In this study, we use a new fluorometric assay to monitor site-specific interactions of promoter DNA and its fragments with holo-RNAP, free σ^{70}, and with the β'-σ^{70} complex. Using this new method, we dissect the energetics of RNAP interaction with the non-template segment of the transcription bubble in the context of oligonucleotide and fork junction model promoter fragments. The results indicate that RNAP binding to the −10 element and to the downstream −6/−3 fragment is highly energetically favorable and can provide a major part of energy required for local promoter melting, whereas interaction with the −2/+2 segment is relatively weak. We show further that formation of the holoenzyme increases the apparent affinity of oligonucleotides mimicking the non-template strand of the transcription bubble by ~300-fold. In contrast, formation of the holoenzyme has only a modest effect on the interaction of σ with shorter non-template oligonucleotides corresponding to the −10 promoter element alone.

EXPERIMENTAL PROCEDURES

Materials—Oligodeoxynucleotides were synthesized by Integrated DNA Technologies. Tetramethylrhodamine-5-maleimide (TMR), BODIPY FL *N*-(2-aminoethyl)maleimide were purchased from Invitrogen, and ATTO 520-maleimide was purchased from ATTO-TEC. *E. coli* RNAP core was purchased from Epicenter.

Plasmids—Plasmid pGEMD(−Cys) encoding a σ^{70} derivative with no Cys residues and plasmid encoding σ^{70} derivative with single Cys residue at position 211 were described previously (17, 18). Plasmid encoding a σ^{70} derivative with a single Cys residue at position 192 and a plasmid encoding a σ^{70} derivative with a single Cys residue at position 211 combined with W434A,W433A substitutions was constructed from plasmid pGEMD(−Cys) by site-directed mutagenesis. Plasmid for overproduction of σ^{70}(104–613) derivative with a single Cys residue at position 211 was constructed by amplifying a DNA fragment encoding amino acids 104–613 of the σ^{70} derivative with appropriate primers introducing NdeI and EcoRI restriction sites at the 5′ and 3′ ends of the fragment, respectively, and cloning the amplified fragment between the NdeI and EcoRI sites of the pET28a expression vector.

Protein Purification and Labeling—Single Cys σ^{70} derivatives were prepared as in Ref. 17. Fluorescent labels were incorporated into single Cys σ^{70} derivatives using Cys-specific chemical modification (procedures as described in Ref. 19), and efficiencies of labeling were >70%. Labeled RNAP holoenzyme derivatives were reconstituted by mixing the RNAP core and labeled σ^{70} at a ratio of 1.2:1, as in Ref. 19. Single Cys σ^{70}(104–613, 211Cys) derivative inclusion bodies were prepared as in Ref. 20, 21 from BL21(DE3) cells carrying pET28a-σ^{70}(104–613, 211Cys) plasmid. The activity of σ^{70} mutants was determined using a fluorometric abortive initiation assay (22) with a 100-bp T5N25 DNA fragment as a template. β' was overexpressed in *E. coli* BL21(λDE3), dissolved in buffer containing 6 M guanidine chloride, and renatured as in Ref. 21. Trypsin digestion reactions contained 2 nM (211Cys-TMR) σ^{70} or (211Cys-TMR, W433A,W434A) σ^{70} and about 0.1 trypsin activity unit per ml in transcription buffer. Reactions were allowed to proceed for 2 h at 25 °C.

DNA Probes—Promoter DNA fragments were formed by mixing equimolar amounts of synthetic complementary strands in a buffer containing 40 mM Tris, pH 7.9, 100 mM NaCl, heating for 2 min at 95 °C, and slowly cooling down to 25 °C.

Fluorometric Assays—Fluorescence measurements were performed using a Quanta-Master QM4 spectrofluorometer (PTI) in transcription buffer (TB: 40 mM Tris-HCl, pH 8.0, 100 mM NaCl, 5% glycerol, 1 mM DTT, and 10 mM $MgCl_2$) containing 0.02% Tween 20 at 25 °C. Final assay mixtures (800 μl) contained 1 nM labeled σ^{70} or RNAP holoenzyme and DNA probes at various concentrations. The (β'-σ^{70}) complex assay mixtures contained 1 nM (211Cys-TMR) σ^{70} and 30 nM β'. The 30 nM β' concentration saturated the fluorescence signal increase in the experiments. Some control experiments were performed using 3 nM labeled free σ^{70} or RNAP holoenzyme. We did not observe a difference between the K_d values measured at either 1 or 3 nM of a beacon concentration. The TMR fluorescence intensities were recorded with an excitation wavelength of 550 nm and an emission wavelength of 578 nm. Kinetic measurements were performed as in Ref. 23.

Data Analysis—To obtain equilibrium dissociation constants (K_d), the experimental dependence of the fluorescent signal amplitude (F) on DNA probe concentration (C) was fit to Equation 1,

$$(1 - X)(C - [\mathrm{RNAP}]X) = K_d X \qquad \text{(Eq. 1)}$$

where $X = (F - F_o)/(F_{max} - F_o)$; F_o is the initial value of the amplitude, and F_{max} is the limiting value of the amplitude at $C = \infty$.

Oligo probes bearing mutations at −7 and −11 positions produced very low fluorescent signal. Dissociation constants of these probes were obtained from competition binding experiments using the consensus single-stranded probe as a ref-

erence. The experiments were carried out at a fixed concentration of a substituted probe and various concentrations of consensus probe. The data were fit to Equation 2,

$$(1 - X)(C - [\text{RNAP}]X) = K_d X(1 + C_0/K_{d,0}) \qquad \text{(Eq. 2)}$$

where $K_{d,0}$ and C_0 are dissociation constant and concentration of the substituted probe, respectively. Equation 2 is valid at $C_0 \gg$ [RNAP], a condition that was fulfilled in our experiments.

Another equilibrium competition binding assay was used to measure affinity of tight RNAP-fork junction complexes (K_d value lower than 0.1 nM). A double-stranded (−58/−14) probe (shown in Fig. 4) producing negligible signal upon binding to (211Cys-TMR) σ^{70} holo-RNAP was used as a competitor. The ratio of equilibrium binding constants for the fork junction probes and the (−58/−14) probe was calculated as described previously (24). The concentrations of fork junctions and (−58/−14) were between 2 and 10 nM. The approach to equilibrium binding was revealed by order of addition experiments as in Ref. 25. Equilibrium binding of (−26/+2)(−26/−12), (−38/−3)(−38/−12)−35mut, and (−38/−7)(−38/−13) probes was reached after incubation at room temperature for 2, 7, and 20 h, respectively. Typical kinetics of reaching equilibrium degree of saturation of RNAP with the (−38/−3)(−38/−12)−35mut and (−58/−14) probes is shown in supplemental Fig. S3.

RESULTS

Design of a Protein Beacon Assay—Tryptophan and tyrosine side chains quench fluorescence of adjacent organic fluorophores (dyes) due to photoinduced electron transfer (PET) between the first excited singlet state of the dye and the ground state of Trp or Tyr (26). Efficient PET usually occurs at length scales below 1 nm. We sought to develop a simple PET-based, one-label quantitative assay to monitor the interaction of bacterial RNAP with promoter DNA. We reasoned that the interaction of the *E. coli* RNAP σ^{70} subunit region 2 with the −10 promoter element might lend itself to such an assay because it is known that this interaction involves multiple aromatic amino acids of σ^{70} region 2.3 that change their environment upon interaction with DNA (27–29). The exact nature of this change is, however, unknown.

Schematic representation of the assay is shown in Fig. 1*A*. The assay is based on measuring emission from a fluorescent label attached to *E. coli* σ^{70} in the vicinity of a cluster of Trp and Tyr residues from conserved region 2.3 (Trp-433, Trp-434, Tyr-425, and Tyr-430). The base-line fluorescence of labeled free σ^{70} or RNAP holoenzyme that contains it is expected to be low due to quenching by the nearby tryptophan and tyrosine residues. Upon DNA binding and establishment of specific interactions with nucleotides from the non-template strand of the −10 promoter element, the contacts between the fluorescent label and residues from the aromatic cluster of σ region 2.3 can become disrupted, which should result in decreased quenching and the enhancement of the fluorescent signal. The assay reports only on protein-DNA interactions confined to small parts of RNAP and DNA adjacent to σ^{70} region 2.3 aromatic residues, *i.e.* on specific interactions important for promoter complex formation. The assay thus should be "blind" to interactions that occur elsewhere in the RNAP molecule. By analogy with previously described molecular and peptide beacons assays (30, 31), we name the new assay a protein (RNAP) beacon assay.

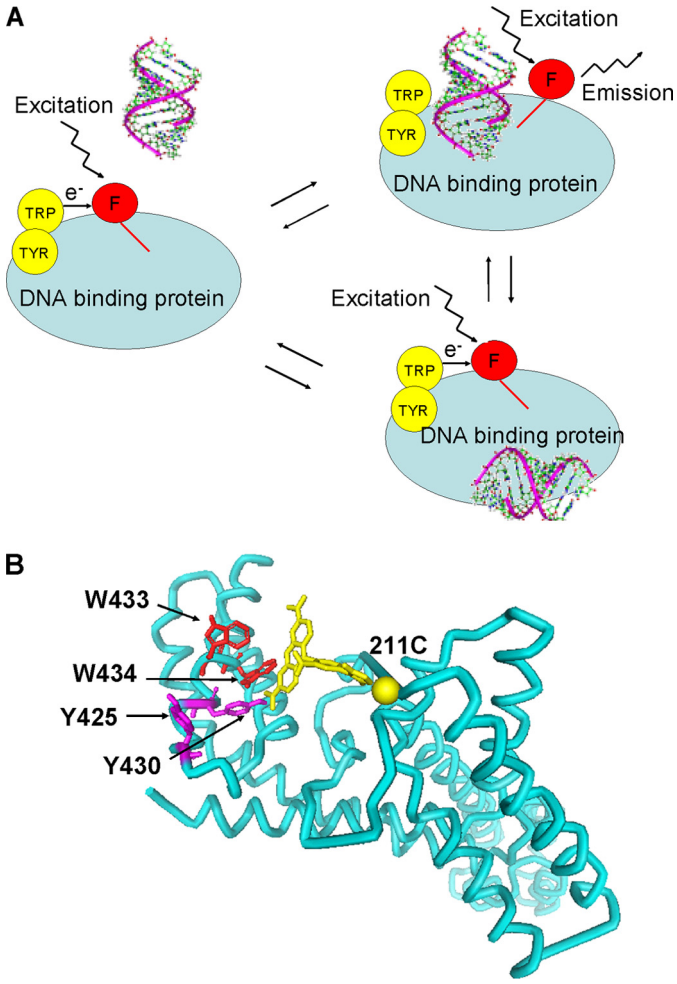

FIGURE 1. **A protein beacon assay to study site-specific interactions of RNAP with promoters or promoter DNA fragments.** *A,* schematic representation of the protein beacon assay. The *red circle* labeled (*F*) indicates the fluorophore; aromatic residues that quench fluorescence in the absence of bound DNA are shown as *yellow circles*. Nonspecific DNA binding at extraneous sites shown at the *bottom* does not affect the fluorescence intensity. *B,* structural model of a fragment of σ^{70} showing the positions of side chains of aromatic residues in region 2.3 and the modeled position of (TMR) fluorophor attached to Cys-211. The structure is from Ref. 29.

Development and Validation of a Protein Beacon Assay—Several previously described functional single cysteine mutants of *E. coli* σ^{70} that allow site-specific introduction of fluorescent labels were prepared. The mutants were chosen based on spatial proximity of modified residues to σ^{70} region 2.3 in available structures containing σ subunits from *E. coli* and *Thermus* spp. (3, 32). A structural model of (211Cys-TMR) σ^{70}, σ^{70} labeled at position 211 with fluorescent label, 5-TMR, is shown in Fig. 1*B* as an example.

RNAP holoenzymes reconstituted from mutant σ labeled with 5-TMR, BODIPY FL, or ATTO-520 (the efficiency of labeling was at least 70%) were functional (at least 80% of the wild-type RNAP activity in abortive initiation assay on the

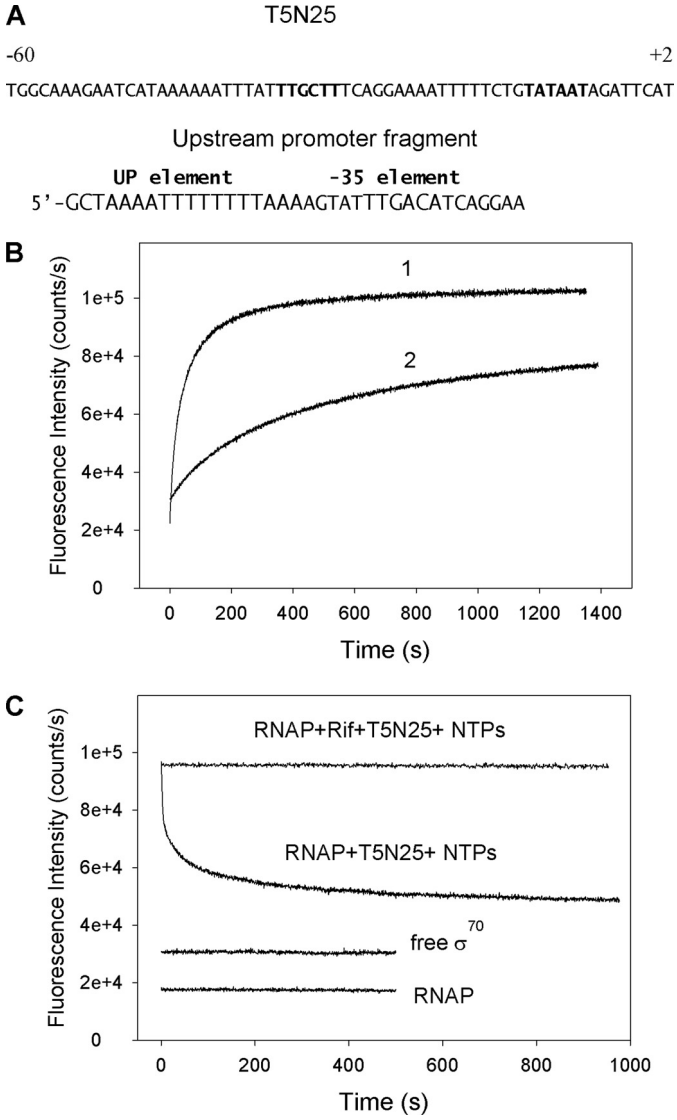

FIGURE 2. **Measuring RNAP-promoter DNA interactions using the protein beacon assay.** *A, top strand* sequences of the T5N25 promoter from position −60 to +2 and the model upstream promoter fragment are shown with the −35 and UP promoter element sequences indicated. *B, curve 1,* time dependence of the increase in fluorescence upon mixing 1 nM (211Cys-TMR) σ^{70} holoenzyme with 2 nM T5N25 DNA fragment. *Curve 2,* same as *curve 1*, but (211Cys-TMR) σ^{70} holoenzyme was preincubated with 100 nM upstream promoter fragment for 5 min prior to the addition of T5N25 DNA. *C,* time-dependent change of the fluorescence signal upon addition of a mixture of ATP, GTP, and UTP (to a final concentration of 0.5 mM each) and 10 nM of unlabeled wild-type σ^{70} to complexes of the T5N25 DNA fragment with (211Cys-TMR) σ^{70} holoenzyme preformed with and without 1 μM rifampicin.

T5N25 promoter). Reconstituted fluorescently labeled RNAP holoenzymes were combined with a double-stranded DNA fragment containing the T5N25 promoter (shown in Fig. 2*A*), and changes in fluorescence were monitored. Upon addition of promoter DNA to RNAP holoenzymes containing mutant σ with 5-TMR attached to residue 192 or 5-TMR, BODIPY FL, or ATTO-520 attached to residue 211, the fluorescent signal increased ~5-fold and saturated in a few minutes. A typical trace, obtained with RNAP holoenzyme containing (211Cys-TMR) σ^{70} and a DNA fragment containing the T5N25 promoter, is shown in Fig. 2*B*. Similar increases were observed when DNA fragments containing the T7 A1 or *lac*UV5 promoters were used. Although the interaction between RNAP holoenzyme beacons and promoter-containing DNA fragments was readily detected at 0.5 nM promoter concentration, no signal increase was observed upon mixing free (211Cys-TMR) σ^{70} with 500 nM promoter fragments, indicating, in agreement with previous data, that free σ^{70} is unable to specifically interact with promoters (1, 2).

Several control experiments were performed to prove that the interaction detected in the protein beacon assay is specific. In one experiment, the interaction of a 35-nt-long double-stranded "upstream" promoter fragment containing the UP element and the −35 element but truncated at position −23 and therefore lacking the −10 promoter element (Fig. 2*A*) with RNAP was studied. Because RNAP elements that can sequence-specifically interact with this fragment are remote from σ region 2.3, the expectation was that RNAP binding to this promoter fragment should not lead to an increase in the fluorescence signal intensity. Indeed, we found that the addition of 100 nM of upstream fragment to RNAP-(211Cys-TMR) σ^{70} resulted in a fluorescence intensity increase that was 10 times lower than that generated by 2 nM of T5N25 promoter DNA (data not shown). The residual weak fluorescence intensity increase may be caused by nonspecific binding of upstream probe to σ^{70} region 2.3. The rate of signal increase caused by the addition of T5N25 promoter DNA to RNAP-(211Cys-TMR) σ^{70} was considerably slowed down by the presence of 100 nM of the upstream fragment (Fig. 2*B*), indicating that this fragment bound RNAP and competed for the binding with T5N25 DNA.

Specific interaction of oligonucleotide whose sequence corresponded to positions −18 to +1 of the λ phage pR′ promoter non-template strand with the σ^{70} holoenzyme was previously reported by Marr and Roberts (8), who used biochemical methods (a gel retardation assay) to show that the interaction is characterized by a K_d of 3 nM and that a substitution of a T at position −12 at the upstream end of the −10 consensus element by a C decreased the interaction 5-fold. We determined dissociation constants for oligonucleotides identical to those used by Marr and Roberts (8) with RNAP beacons based on (211Cys-TMR) σ^{70}, (211Cys-BODIPY FL) σ^{70}, and (192Cys-TMR) σ^{70} (supplemental Fig. S1 and supplemental Table S1). Although dissociation constants for "wild-type" oligo C (K_d(C)) and mutant oligo M K_d(M) varied within a factor of 5 (from 6.2 to 28.8 nM for oligo C) for different beacons, individual K_d(M)/K_d(C) ratios were close to 4 for every beacon tested (supplemental Table S1). The ratios of K_d values are in good agreement with the Marr and Roberts data (8). The differences in apparent binding constant values observed with individual beacons and in gel retardation assay could be at least partially due to the fact that some part of free energy of oligonucleotide binding must be used to disrupt the van der Waals interaction of the fluorophore with the quencher. If so, then dissociation constants calculated using the beacon assay are expected to be somewhat higher than the actual values for unmodified RNAP, as is indeed observed. An oligo that contained nucleotides most rarely found at each position of the −10 hexamer (oligo A of Marr and Roberts (8)) did not generate any sig-

nal (supplemental Fig. S1). The K_d value for oligo A was determined from a competition binding experiment with oligo C as a reference and found to be 15-fold lower than K_d for oligo C.

Precise quantification of partial contributions of region 2.3 aromatic residues to fluorescence quenching is complicated by their involvement in the −10 element binding (27–29). We found that (211Cys-TMR) σ^{70} holoenzyme carrying a double substitution of Trp-433 and Trp-444 to Ala exhibited less than 10% increased fluorescence in the presence of 200 nM promoter DNA (data not shown). The absence of increased fluorescence was not caused by the inability of the holoenzyme carrying fluorescently labeled W433A,W434A σ^{70} to bind to promoter DNA, as evidenced by gel retardation analysis (data not shown), and is in agreement with the fact that a σ^{70} RNAP mutant bearing four amino acid substitutions W433A, W434A, F427A, and Y430A forms complexes that resemble those formed by wild-type RNAP (33). Trypsin digestion of (211Cys-TMR) σ^{70} enhanced the TMR fluorescence intensity 3.8-fold (data not shown), which can be explained by breaking of TMR contacts with the aromatic residue quenchers. In contrast, similar digestion of (211Cys-TMR, W433A,W434A) σ^{70} resulted in only 8% signal increase. These results indicate that Trp-433 and Trp-434 indeed play an important role in the 211Cys-TMR fluorescence quenching.

If increased fluorescence observed in the presence of promoter DNA were due to formation of promoter complexes, then a decrease in fluorescence intensity should be observed upon RNAP escape from promoter into elongation. To test this prediction, nucleotide triphosphates and unlabeled σ^{70} (10-fold excess as compared with the labeled σ^{70} protein) were added to preincubated reactions containing fluorescent RNAP holoenzyme and promoter DNA (Fig. 2*C*). Unlabeled σ^{70} was added to prevent recapturing of dissociated fluorescently labeled σ by the core, which could have led to reformation of promoter complexes with fluorescently labeled holoenzyme. As can be seen, fluorescence decreased upon the addition of nucleotide triphosphates and unlabeled σ by 2.5-fold. This effect was not observed in the presence of 1 μM Rifampicin, a drug that prevents RNAP escape from promoter. We interpret this result as suggesting that a decrease in fluorescence in the absence of rifampicin is due to RNAP leaving the promoter, which leads to disruption of σ contacts with DNA.

Based on the data presented above, we conclude that our PET-based protein beacon assay is behaving as expected from design and that RNAP holoenzymes containing fluorescently labeled σ^{70} provide a simple, quantitative, and real time assay to measure RNAP interactions with promoter DNA.

In what follows, we use the protein beacon assay to study the interaction of model promoter fragments with RNAP holoenzyme, the β'-σ^{70} complex, and free σ^{70}. Data for beacons based on (211Cys-TMR) σ^{70} are presented because these beacons generated the highest signal intensity upon DNA interaction in the context of both RNAP holoenzyme, the β'-σ^{70} complex, and free σ^{70}.

Interactions of RNAP Holoenzyme and Free σ^{70} with Oligos Containing the −10 Promoter Element Sequence—As a starting point, oligonucleotide corresponding to nontranscribed strand positions −12/+2 of the T5N25 promoter was used (Fig. 3*A*). Four "mutant" −12/+2 oligos containing substitutions at positions −7, −9, −10, and −11 (−12/+2; −7C, −12/+2; −9C, −12/+2; −10G and, −12/+2; −11C, correspondingly) were used as controls. We found that the wild-type oligo bound RNAP containing (211Cys-TMR) σ^{70} with the highest affinity (K_d = 0.15 μM), whereas oligos with substitutions at highly conserved positions −11 and −7 bound poorly (Fig. 3*B* and Table 1). The −12/+2 oligo bound free (211Cys-TMR) σ^{70} 280 times more weakly than the holoenzyme (K_d = 41 μM, see Fig. 3*D* and Table 1). The binding, however, was specific, because binding of free σ^{70} to mutant oligos showed sequence dependence similar to that found for holo-RNAP (Table 1).

The efficiency of free σ^{70} and RNAP holoenzyme interactions with even shorter oligos corresponding to T5N25 promoter positions −12/−3 and −12/−6 (Fig. 3*A*) was determined next (Fig. 3, *B–D* and Table 2). Corresponding mutant oligos with substitution of T in position −7 for C were used as controls. For free σ, the following results were obtained (Fig. 3*D* and Table 2). The −12/−3 oligo bound as efficiently as the −12/+2 oligo ($K_d \approx 40$ μM), indicating that non-template DNA nucleotides downstream of position −3 do not contribute to σ binding. The binding avidity of the −12/−6 oligo was ~5-fold lower (K_d = 220 μM). In all cases, the binding was specific as it was severely affected by substitutions in the −11 and −7 positions. The −12/−3 and −12/−6 oligos bound the holoenzyme with ~10 and ~500-fold lower affinity than the −12/+2 oligo (Fig. 3, *B* and *C*, and Table 2). The −12/−7 oligo, which corresponded exactly to the −10 promoter element TATAAT, was also tested and was found to bind both free σ^{70} and holo-RNAP poorly; in fact, we could not achieve saturation (data not shown).

It is instructive to compare ratios of dissociation constants for complexes formed by free σ^{70} and RNAP holoenzyme with promoter oligos of the same length (Table 2). The shortest oligo, containing the entire −10 promoter element and one downstream nucleotide, oligo −12/−6, binds the holoenzyme only 2.8 times better than free σ^{70}. An oligo of intermediate length (−12/−3) binds the holoenzyme 29 times better than free σ^{70}. The longest oligo of the set, the −12/+2 oligo, binds ~300 times more avidly to RNAP holoenzyme than to σ^{70}. In other words, the shorter the oligo containing the −10 promoter element sequence, the less the difference between the efficiency of its binding to free σ and the holoenzyme. This result suggests that the much stronger binding of the −12/+2 oligo to the holoenzyme than to σ^{70} mainly results from interactions outside of the −10 element and may involve RNAP core subunits or regions of σ^{70} other than region 2.

Interactions of RNAP Holoenzyme and Free σ^{70} with Fork Junction Probes—Holo-RNAP specifically binds fork junction DNAs, model promoter substrates containing double-stranded upstream DNA, and single-stranded extensions corresponding to the non-template strand of the −10 promoter element (34). We evaluated free energy (ΔG) of RNAP inter-

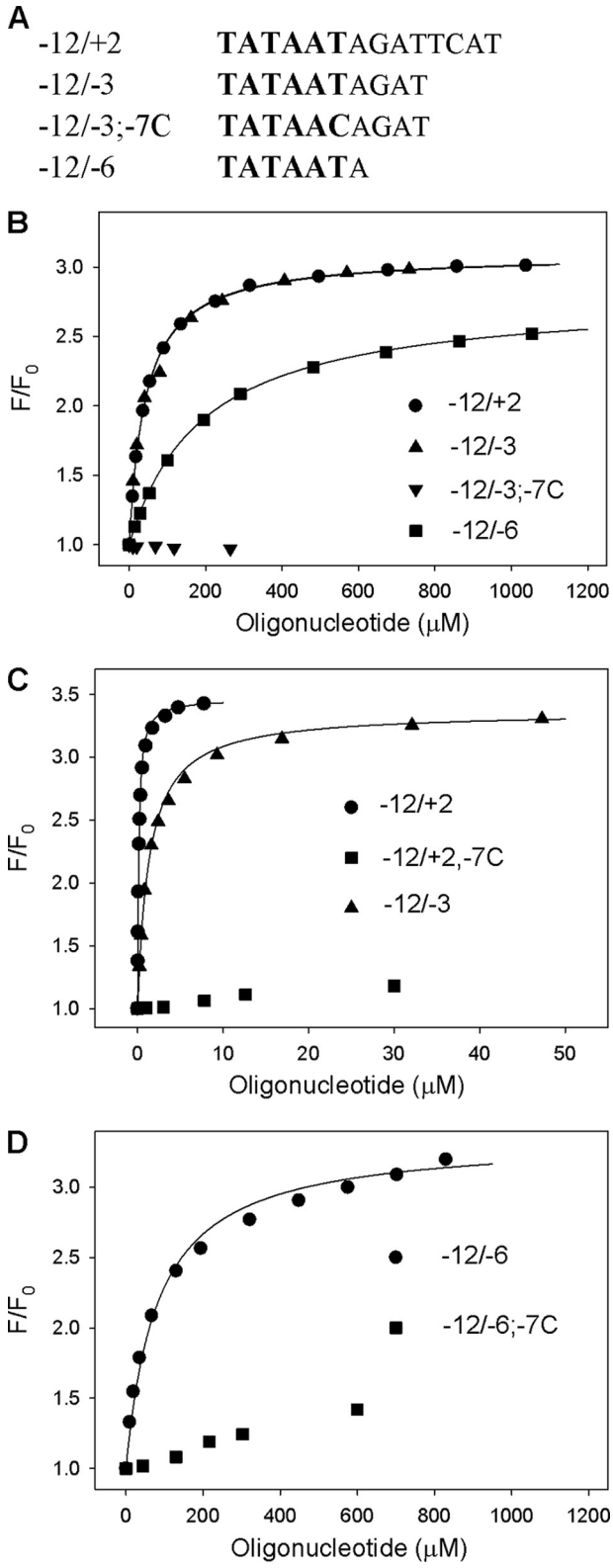

FIGURE 3. **Binding of non-template oligos containing the −10 promoter element consensus sequence to free σ^{70} and holo-RNAP.** *A,* sequences of oligos −12/+2, −12/−3, −12/−3, 7C, and −12/−6 are shown with the −10 promoter element sequence in *larger size font*. *B,* titration of free (211Cys-TMR) σ^{70} with −12/+2, −12/−3, −12/−6, and −12/−3; 7C oligos. *C,* titration of (211Cys-TMR) σ^{70} holoenzyme with −12/+2, −12/−3, and −12/+2; 7C oligos. *D,* titration of (211Cys-TMR) σ^{70} holoenzyme with −12/−6 and −12/−6; 7C oligos. For all data panels, the *solid lines* correspond to a nonlinear regression fit of the data to Equation 1 (see "Experimental Procedures").

TABLE 1

Dissociation constants for the binding of sequence-substituted derivatives of −12/+2 oligos to free σ^{70} and the RNAP holoenzyme

The K_d values presented are averages obtained from 2 to 3 individual experiments, the error is ±15%.

Oligo	K_d, free σ	K_d, holo-RNAP
	μM	μM
−12/+2	41	0.15
−12/+2; −7C	>700	70
−12/+2; −9C	500	2.1
−12/+2; −10A	130	0.6
−12/+2; −11C	>700	30

action with the −12/−7, −6/−3, and −2/+2 segments of the non-template strand of the transcription bubble in the context of fork junction DNA probes based on the T5N25 promoter sequence (shown in Fig. 4). The RNAP interactions with the −2/+2 segment were also studied using fork junction probes based on the *lac*UV5 promoter sequence. The $\Delta G_{-12/-7}$,$\Delta G_{-6/-3}$, and $\Delta G_{-2/+2}$ values were quantified by comparing K_d values of a fork junction probe bearing a single-stranded segment of interest with a K_d values of a similar probe that lacked such a segment. Such measurements could not be carried out using probes with identical upstream double-stranded fragments because K_d values for probes with the shortest and longest single-stranded segments differ more than 10^7-fold. Therefore, probe affinities were adjusted by making changes in the sequence and/or shortening the double-stranded segment.

RNAP binding to several fork junctions was found to be very strong (K_d <0.1 nM). We measured the K_d value of such tight complexes using an equilibrium competition binding assay. A double-stranded model promoter fragment containing the consensus UP element, the −35 element, and the TG motif of the extended −10 element was used as a competitor ((−58/−14) probe, shown in supplemental Fig. S3*A*). Upon binding to the holo-RNAP beacon, the (−58/−14) probe generates a negligible signal. Yet the binding of this probe is very tight (K_d = 0.015 nM) as revealed by a competition binding experiments using the (−58/−14) probe and other probes, for which K_d values were determined by titration.

Equilibrium dissociation constants of RNAP holoenzyme complexes with the set of probes described above are shown in Table 3. As can be seen, the −7/−12 single-stranded segment increased the binding to RNAP by ~30,000-fold. A fork junction containing a single-stranded extension up to position −3 bound ~200-fold better than the corresponding probe extending to position −7. Finally, extension of the single-stranded segment to position +2 increased the binding efficiency ~10-fold, compared with the template extending to position −3 (the latter result was obtained on both T5N25 and *lac*UV5-based probes). We conclude that the data on dissection of the energetics of RNAP interaction with the transcription bubble non-template stand obtained with the oligonucleotide and fork junction model promoter fragments indicate that RNAP binding to the to the −10 element and to a segment immediately adjacent to the −10 element is quite strong, whereas the downstream segment interacts comparatively weakly.

TABLE 2

Dissociation constants for the binding of −10 oligos to free σ^{70}, σ^{70} RNAP holoenzyme, and the (β'-σ^{70}) complex

The K_d values presented are averages from 2 to 3 individual experiments, the error is ±15%.

Oligo	K_d, free σ	K_d holo-RNAP	K_d (β'-σ)	K_d (σ)/K_d (holo)	K_d (σ)/K_d (β'-σ)
	μM	μM	μM		
−12/+2	41	0.15	5.1	270	8
−12/−3	43	1.5	8.7	29	4.9
−12/−6	220	80	110	2.8	2
*lac*UV5, −18 + 1	37		0.4		93

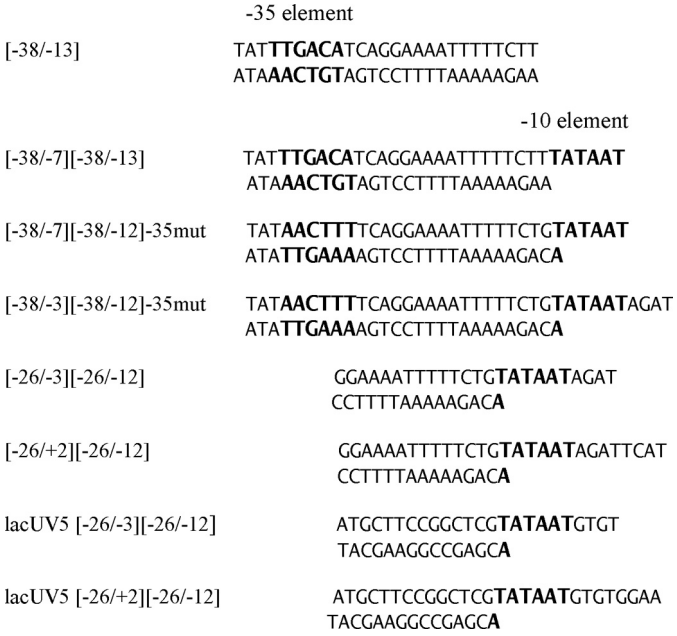

FIGURE 4. **Fork junction and double-stranded promoter fragment DNA sequences.** *Numbers in brackets* correspond to borders of upper and bottom strands of fork junction probes with respect to the transcription start position (+1); *−35mut* stands for mutated sequence of the −35 element.

The binding of free (211Cys-TMR) σ^{70} to fork junction probes was also measured using the protein beacon assay. The fork junctions DNA probes used in these experiments are shown in supplemental Fig. S2*A*. These probes are identical, but one of them contains a TG motif of the extended −10 element. The affinities of free (211Cys-TMR) σ^{70} to the fork junction probes were somewhat lower than those found for the −12/−3 oligo (K_d~100 μM; supplemental Fig. S2*B*). The interaction, however, was specific, because substitutions in the single-stranded part of the fork junction template that decreased the similarity to the −10 element consensus sequence decreased the binding. The presence of the TG motif had no effect on the binding affinity of (211Cys-TMR) σ^{70}, indicating that free σ is unable to recognize this element, at least in the context of fork junction probes.

Interactions of the β'-σ^{70} Complex with Model Promoter Fragments—The main site of σ^{70} interaction with the RNAP core enzyme is located in the β' subunit (35). The interaction is thought to cause conformational changes in σ^{70} that affect its ability to interact with DNA. Thus, Young *et al.* (14) demonstrated using photocross-linking and LRET techniques that β' or a short β' fragment that binds σ is sufficient to induce detectable binding of σ to −18/+1 and −13/+1 *lac*UV5 nontemplate strand oligos. The binding of isolated σ^{70} to oligos was not detectable by the method used. We measured K_d values for the binding of our set of −10 oligos as well as the *lac*UV5 −18/+1 non-template strand oligo used by Young *et al.* (14) to the β'-σ^{70} complex (Table 2). In agreement with earlier data, β' induced a very significant, 90-fold, increase in the interaction with the *lac*UV5 −18/+1 oligo. On the other hand, K_d values for β'-σ^{70} complex interaction with −12/+2, −12/−3, and −12/−6 oligos were comparable with those obtained with free σ, with the strongest stimulation (for −2/+2 oligo) being less than 10-fold. The result suggests that there exist favorable interactions between the β'-σ^{70} complex and the upstream segment of the *lac*UV5 −18/+1 oligo.

The β'-σ^{70} complex binding to three fork junction probes containing various upstream fragments was also studied. The three probes (Fig. 5*A*) were designed to reveal if there are any specific interactions between β'-σ^{70} and the −35 consensus element and the TG motif of extended −10 promoter element. Comparison of data in Fig. 5*B* and Table 2 shows that β'-σ^{70} binds fork junctions much more effectively than the −12/−3 oligonucleotide, pointing toward the existence of strong favorable interactions between β'-σ^{70} and upstream double-stranded DNA. The highest affinity of the −35 consensus; TG probe demonstrates the ability of β'-σ^{70} to recognize the extended −10 element. On the other hand, a small difference in the binding to the −35 cpnsensus and −35 mutant probes indicates that the β'-σ^{70} complex is unable to recognize the −35 element, at least in the context of a fork junction probe.

Interactions of Free σ^{70} Lacking Region 1 and the Corresponding RNAP Holoenzyme with Model Promoter Templates—The N-terminal conserved region 1 of σ^{70} is thought to modulate RNAP holoenzyme interactions with DNA. Region 1.1 is thought to occupy an RNAP trough where double-stranded DNA downstream of the transcription initiation start point is bound in the open promoter complex (17, 36). We prepared protein beacons based on σ^{70} truncated at position 104 ((104–613, 211Cys-TMR) lacks the entire region 1.1 and part of region 1.2) to determine the contribution of conserved region 1 to the binding of oligo and fork junction promoter fragments. The mutant σ bound oligos with avidity similar to that of the wild-type σ^{70} (Fig. 6 and Table 4). However, in sharp contrast with the data obtained with RNAP containing full-size σ^{70} beacons (Fig. 3), (104–613, 211Cys-TMR) σ^{70} holo-RNAP bound the −12/−6, −12/−3, and −12/+2 oligos with similar affinities that were nearly indistinguishable from free (104–613, 211Cys-TMR) σ^{70} binding affinities (Fig. 6 and Table 4). A similar finding was reported by Zenkin *et al.* (20). The observations thus seem to suggest that σ^{70} region 1 is involved, directly or indirectly, in favorable interactions

TABLE 3

Interaction of RNAP holoenzyme with fork junction probes

Free energy of RNAP binding to the −12/−7, −12/−3, and −2+/2 single-stranded segments calculated using equation $\Delta G = -RT \ln(K_d(\mathbf{1})/_d(\mathbf{2}))$.

Assayed segment	Probe	K_d	K_d (1)/K_d (2)	$-\Delta G$	$-\Delta G$/base
		nM		*kcal/mol*	*kcal/mol*
−12/−7	**1,** [−38/−13]	170	28,000	6.1	1.02
	2, [38/−7][−38/−13]	0.0061			
−6/−3	**1,** [−38/−7][−38/−12]−35mut	2.1			
	2, [−38/−3][−38/−12]−35mut	0.01	210	3.2	0.80
−2/+2	**1,** [−26/−3][−26/−12]	0.46			
	2, [−26/+2][−26/−12]	0.05	9.2	1.3	0.33
	1, lacUV5[−26/−3][−26/−12]	5.3	13	1.5	0.38
	2, lacUV5[−26/+2][−26/−12]	0.39			

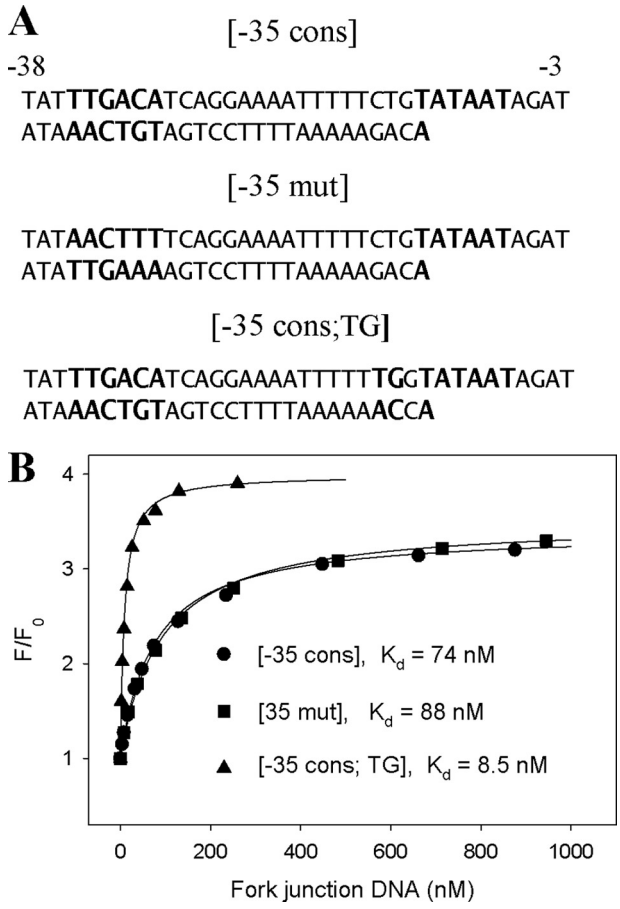

FIGURE 5. **Binding of fork junction DNA probes to the β'-σ^{70} complex.** *A,* sequence of the fork junction probes with the consensus extended −10 and −35 promoter element sequences in *larger size font. B,* titration of the β'-(211Cys-TMR) σ^{70} complex with the fork junction probes. The *solid lines* correspond to a nonlinear regression fit of the data to Equation 1.

with non-template DNA downstream of the −10 promoter element.

We also measured affinity of the mutant holo-RNAP beacon to (−38/−7)(−38/−12)−35mut and (−38/−3)(−38/−12)−35mut fork junction probes (shown in Fig. 4) as well as to upstream double-stranded DNA probe (−38–12)TG (Table 5). The data show that the binding of fork junctions to mutant RNAP is considerably weaker than to wild-type RNAP, in agreement with previous results (20). Compared with the wild-type holoenzyme, the 45-fold deterioration of the (−38/−7)(−38/−12)-35mut fork junction avidity conferred by the region 1 truncation is noticeably higher than the 4-fold decrease in the affinity to the −12/−6 oligo (Tables 2, 4, and 5). This difference may be explained in part by the overall reduction of mutant RNAP affinity to the double-stranded segment of fork junction probes: indeed, (104–613, 211Cys-TMR) σ^{70} holoenzyme bound the double-stranded (−38–12)TG probe 4.7 less efficiently than the wild-type holoenzyme (Table 5).

DISCUSSION

Interactions of holo-RNAP with promoter elements have been extensively analyzed using oligonucleotides and fork junction model templates (8, 33, 37). Zenkin *et al.* (20) have recently shown that, in contrast to previous studies, specific interaction between free σ^{70} and the −10 element oligonucleotides can also be detected at high (>1.5 μM) oligo concentration. In this study, we applied a new fluorometric assay to quantitative investigation of the interaction between free σ^{70} and the −10 element oligonucleotides. We found that free σ^{70} interacts with the −12/−3 segment of non-template promoter strand. No interaction with other promoter segments in the context of oligonucleotides and fork junction probes as well as with full promoter DNA was detected.

Formation of the holoenzyme increases the apparent affinity of oligonucleotides mimicking the non-template strand of the transcription bubble by ~300-fold. However, this increase is mainly a consequence of binding to bases outside of the −10 element. This result is incompatible with a model that envisions a drastic improvement of specific recognition of the −10 promoter element by σ upon the holoenzyme formation as the main reason for highly efficient promoter recognition by the RNAP holoenzyme.

Our data on dissecting the interactions between RNAP and the transcription bubble non-template stand in the context of oligonucleotide and fork junction promoter probes indicate that RNAP binding to the −10 element and to single-stranded segment located immediately downstream is highly energetically favorable, whereas the interactions with DNA further downstream, around the transcription start point, are weak. This result provides a rationale for biochemical data indicating that on several promoters the downstream part of the transcription bubble melts later than the upstream part, which includes the −10 element (38–41). On the other hand, a single molecule study (42) and recent work from Record and co-workers (43) suggested that DNA melting and unwinding occurred in a single step during open promoter complex for-

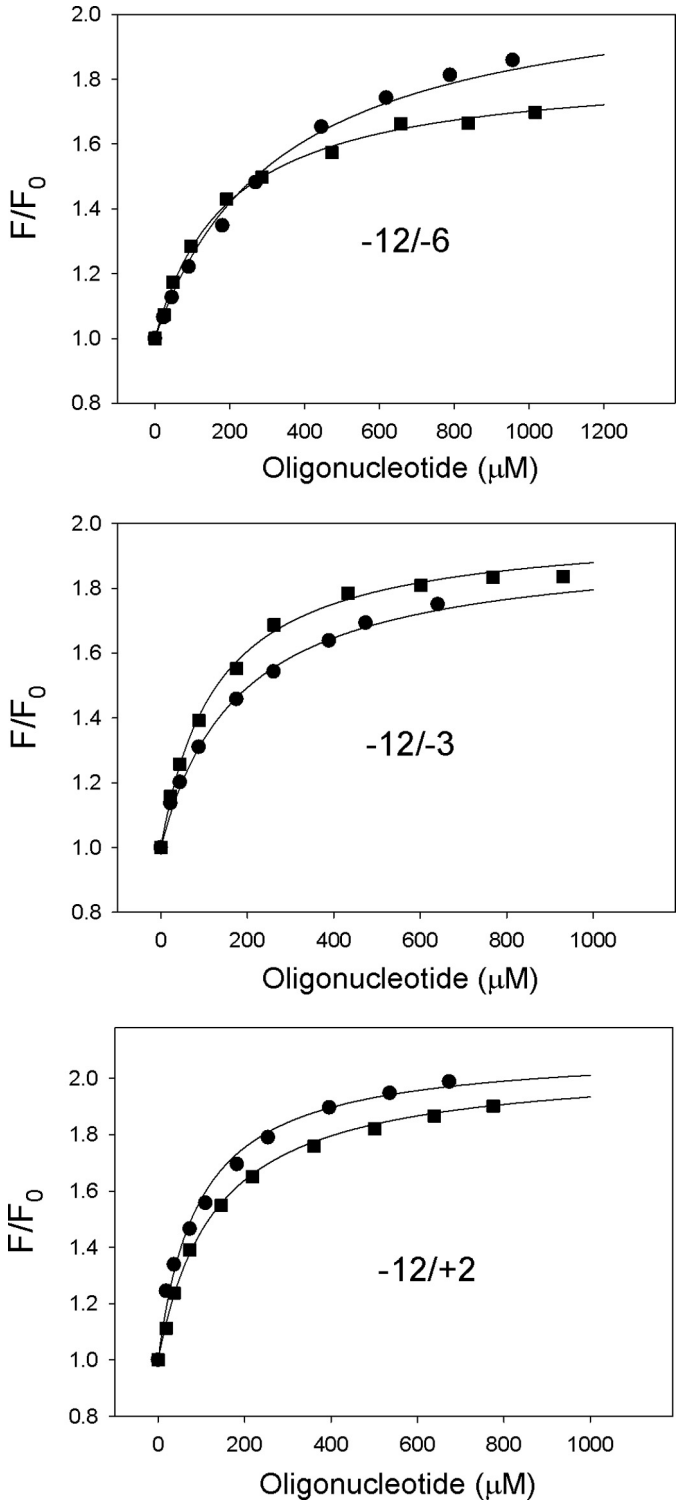

FIGURE 6. **Binding of non-template oligos containing the −10 promoter element consensus sequence to holo-RNAP containing (104–613) σ^{70} and free (104–613) σ^{70}.** The data panels show titration of free (211Cys-TMR, 104–613) σ^{70} (*squares*) and (211Cys-TMR, 104–613) σ^{70} holoenzyme (*circles*) with −12/−6, −12/−3, and −12/+2 oligos. Sequences of the oligos are shown in Fig. 3. For all data panels, the *solid lines* correspond to a nonlinear regression fit of the data to Equation 1.

mation. Clearly, additional experiments employing methods with high temporal resolution will be needed to resolve this issue. It is also probable that the melting pathway may be different on different promoters.

TABLE 4

Dissociation constants for the binding of −12/+2, −12/−3, and −12/−6 oligos to free [104–613] σ^{70} and the [104–613] σ^{70} RNAP holoenzyme

The K_d values shown are averages obtained from 2 to 3 individual experiments, the error is ± 25%.

Oligo	K_d, free σ	K_d, holo-RNAP	K_d (σ)/K_d (holo)
	μM	μM	
−12/+2	130	94	1.4
−12/−3	130	180	0.72
−12/−6	200	330	0.61

TABLE 5

Dissociation constants for the binding of fork junction and double-stranded promoter fragments to the RNAP holoenzymes containing [104–613, 211Cys-TMR] σ^{70} and full-length σ^{70} [211Cys-TMR] (σ_{FL})

The structures of [−38/−7][−38/−12]−35 mut and [−38/−3][−38/−12]−35 mut are shown in Fig. 4; [−38/−12]TG corresponds to the double-stranded fragment of the [−35cons]TG probe shown in Fig. 5*A*. The K_d values shown are averages obtained from 2 to 3 individual experiments; the error is ±15%.

DNA probe	K_d, $\sigma_{104-613}$ RNAP	K_d, σ_{FL} RNAP	K_d, $\sigma_{104-613}$ RNAP/K_d, σ_{FL} RNAP
	nM	nM	
[−38/−7][−38/−12]−35 mut	95	2.1	45
[−38/−3][−38/−12]−35 mut	7.6	0.01	760
[−38/−12]TG	57	12	4.7

A highly conserved part of σ^{70} region 1, region 1.2, interacts with a promoter segment located immediately downstream of the −10 element (10, 20, 44). In the protein beacon assay, the presence of the −6/−3 single-stranded segment increased the binding affinity of wild-type RNAP holoenzyme 210-fold (Table 3). In contrast, only ~12-fold stimulation was obtained when the RNAP mutant lacking σ region 1.1 and a part of region 1.2 was used (Table 5). The residual stimulation may be due to the binding of σ region 1.2 or may be caused by other interactions, possibly involving RNAP core subunits (11).

The deletions of σ^{70} N-terminal fragments containing region 1 are known to relieve the autoinhibition of free σ^{70} binding to double-stranded DNA fragments containing promoter sequences (46). However, in our work, we did not detect improved binding of short oligos to the (104–613, 211Cys-TMR) σ^{70}. This discrepancy may be explained by increased nonspecific DNA binding to free σ^{70} without region 1, as was indeed observed (46). In contrast, the beacon assay selectively reports on specific σ^{70} interactions with the −10 promoter element, which appear to be independent of region 1.

In contrast to free σ^{70}, the β'-σ^{70} complex has noticeable affinity to fork junction probes. As seen from Fig. 5, the TG segment of the extended −10 element improves binding of a fork junction probe to β'-σ^{70} ~9-fold. Thus, the β' interaction with σ^{70} relieves the autoinhibition effect, which prevents the TG motif interaction with σ^{70} region 3.0 in the context of free σ^{70}. The recognition of the TG motif by a minimal RNAP-melting fragment assembled from the N terminus of the β' subunit (amino acids 1–314) and amino acids 94–507 of the σ^{70} subunit was previously observed (45). However the minimal melting fragment lacks σ^{70} segments, which can be involved in the autoinhibition of σ^{70}-DNA interactions (46), complicating interpretation of TG motif interactions with the

RNAP minimal melting fragment. The inability of the β'-σ^{70} complex to recognize the −35 element in the context of the fork junction probes is in agreement with previous structural and biochemical studies showing an important role of the β flap domain in formation of holo-RNAP conformation able to bind the −35 element in the context of promoter DNA (16, 47, 48).

In summary, our work shows that the protein beacon method developed here allows one to measure various RNAP promoter interactions spanning a K_d range from picomolar to nearly millimolar. The assay can be instrumental in systematic quantitative dissection of fine details of RNAP interactions with promoters.

REFERENCES

1. Burgess, R. R., Travers, A. A., Dunn, J. J., and Bautz, E. K. (1969) *Nature* **221,** 43–46
2. Gross, C. A., Chan, C., Dombroski, A., Gruber, T., Sharp, M., Tupy, J., and Young, B. (1998) *Cold Spring Harbor Symp. Quant. Biol.* **63,** 141–155
3. Campbell, E. A., Muzzin, O., Chlenov, M., Sun, J. L., Olson, C. A., Weinman, O., Trester-Zedlitz, M. L., and Darst, S. A. (2002) *Mol. Cell* **9,** 527–539
4. Barne, K. A., Bown, J. A., Busby, S. J., and Minchin, S. D. (1997) *EMBO J.* **16,** 4034–4040
5. Feklistov, A., Barinova, N., Sevostyanova, A., Heyduk, E., Bass, I., Vvedenskaya, I., Kuznedelov, K., Merkiene, E., Stavrovskaya, E., Klimasauskas, S., Nikiforov, V., Heyduk, T., Severinov, K., and Kulbachinskiy, A. (2006) *Mol. Cell* **23,** 97–107
6. deHaseth, P. L., Zupancic, M. L., and Record, M. T., Jr. (1998) *J. Bacteriol.* **180,** 3019–3025
7. Roberts, C. W., and Roberts, J. W. (1996) *Cell* **86,** 495–501
8. Marr, M. T., and Roberts, J. W. (1997) *Science* **276,** 1258–1260
9. Lim, H. M., Lee, H. J., Roy, S., and Adhya, S. (2001) *Proc. Natl. Acad. Sci. U.S.A.* **98,** 14849–14852
10. Haugen, S. P., Berkmen, M. B., Ross, W., Gaal, T., Ward, C., and Gourse, R. L. (2006) *Cell* **16,** 1069–1082
11. Naryshkin, N., Revyakin, A., Kim, Y., Mekler, V., and Ebright, R. H. (2000) *Cell* **101,** 601–611
12. Fenton, M. S., and Gralla, J. D. (2003) *J. Biol. Chem.* **278,** 39669–39674
13. Kulbachinskiy, A., Mustaev, A., Goldfarb, A., and Nikiforov, V. (1999) *FEBS Lett.* **454,** 71–74
14. Young, B. A., Anthony, L. C., Gruber, T. M., Arthur, T. M., Heyduk, E., Lu, C. Z., Sharp, M. M., Heyduk, T., Burgess, R. R., and Gross, C. A. (2001) *Cell* **105,** 935–944
15. Callaci, S., Heyduk, E., and Heyduk, T. (1999) *Mol. Cell* **3,** 229–238
16. Kuznedelov, K., Minakhin, L., Niedziela-Majka, A., Dove, S. L., Rogulja, D., Nickels, B. E., Hochschild, A., Heyduk, T., and Severinov, K. (2002) *Science* **295,** 855–857
17. Mekler, V., Kortkhonjia, E., Mukhopadhyay, J., Knight, J., Revyakin, A., Kapanidis, A. N., Niu, W., Ebright, Y. W., Levy, R., and Ebright, R. H. (2002) *Cell* **108,** 599–614
18. Owens, J. T., Miyake, R., Murakami, K., Chmura, A. J., Fujita, N., Ishihama, A., and Meares, C. F. (1998) *Proc. Natl. Acad. Sci. U.S.A.* **95,** 6021–6026
19. Mukhopadhyay, J., Kapanidis, A. N., Mekler, V., Kortkhonjia, E., Ebright, Y. W., and Ebright, R. H. (2001) *Cell* **106,** 453–463
20. Zenkin, N., Kulbachinskiy, A., Yuzenkova, Y., Mustaev, A., Bass, I., Severinov, K., and Brodolin, K. (2007) *EMBO J.* **26,** 955–964
21. Borukhov, S., and Goldfarb, A. (1993) *Protein Expr. Purif.* **4,** 503–511
22. Callaci, S., and Heyduk, T. (1998) *Biochemistry* **37,** 3312–3320
23. Feklistov, A., Mekler, V., Jiang, Q., Westblade, L. F., Irschik, H., Jansen, R., Mustaev, A., Darst, S. A., and Ebright, R. H. (2008) *Proc. Natl. Acad. Sci. U.S.A.* **105,** 14820–14825
24. Matlock, D. L., and Heyduk, T. (2000) *Biochemistry* **39,** 12274–12283
25. Nickels, B. E., Garrity, S. J., Mekler, V., Minakhin, L., Severinov, K., Ebright, R. H., and Hochschild, A. (2005) *Proc. Natl. Acad. Sci. U.S.A.* **102,** 4488–4493
26. Doose, S., Neuweiler, H., and Sauer, M. (2005) *Chemphyschem.* **6,** 2277–2285
27. Fenton, M. S., Lee, S. J., and Gralla, J. D. (2000) *EMBO J.* **19,** 1130–1137
28. Tomsic, M., Tsujikawa, L., Panaghie, G., Wang, Y., Azok, J., and deHaseth, P. L. (2001) *J. Biol. Chem.* **276,** 31891–31896
29. Schroeder, L. A., Gries, T. J., Saecker, R. M., Record, M. T., Jr., Harris, M. E., and DeHaseth, P. L. (2009) *J. Mol. Biol.* **385,** 339–349
30. Tyagi, S., and Kramer, F. R. (1996) *Nat. Biotechnol.* **14,** 303–308
31. Oh, K. J., Cash, K. J., Hugenberg, V., and Plaxco, K. W. (2007) *Bioconjug. Chem.* **18,** 607–609
32. Malhotra, A., Severinova, E., and Darst, S. A. (1996) *Cell* **87,** 127–136
33. Sun, L., Dove, S. L., Panaghie, G., deHaseth, P. L., and Hochschild, A. (2004) *J. Mol. Biol.* **343,** 1171–1182
34. Guo, Y., and Gralla, J. D. (1998) *Proc. Natl. Acad. Sci. U.S.A.* **95,** 11655–11660
35. Arthur, T. M., and Burgess, R. R. (1998) *J. Biol. Chem.* **273,** 31381–31387
36. Murakami, K. S., and Darst, S. A. (2003) *Curr. Opin. Struct. Biol.* **13,** 31–39
37. deHaseth, P. L., and Tsujikawa, L. (2003) *Methods Enzymol.* **370,** 553–567
38. Zaychikov, E., Denissova, L., Meier, T., Götte, M., and Heumann, H. (1997) *J. Biol. Chem.* **272,** 2259–2267
39. Auner, H., Buckle, M., Deufel, A., Kutateladze, T., Lazarus, L., Mavathur, R., Muskhelishvili, G., Pemberton, I., Schneider, R., and Travers, A. (2003) *J. Mol. Biol.* **331,** 331–344
40. Figueroa-Bossi, N., Guérin, M., Rahmouni, R., Leng, M., and Bossi, L. (1998) *EMBO J.* **17,** 2359–2367
41. Rogozina, A., Zaychikov, E., Buckle, M., Heumann, H., and Sclavi, B. (2009) *Nucleic Acids Res.* **37,** 5390–5404
42. Revyakin, A., Ebright, R. H., and Strick, T. R. (2004) *Proc. Natl. Acad. Sci. U.S.A.* **101,** 4776–4780
43. Gries, T. J., Kontur, W. S., Capp, M. W., Saecker, R. M., and Record, M. T., Jr. (2010) *Proc. Natl. Acad. Sci. U.S.A.* **107,** 10418–10423
44. Haugen, S. P., Ross, W., Manrique, M., and Gourse, R. L. (2008) *Proc. Natl. Acad. Sci. U.S.A.* **105,** 3292–3297
45. Young, B. A., Gruber, T. M., and Gross, C. A. (2004) *Science* **203,** 1382–1384
46. Dombroski, A. J., Walter, W. A., Record, M. T., Jr., Siegele, D. A., and Gross, C. A. (1992) *Cell* **70,** 501–512
47. Murakami, K. S., Masuda, S., Campbell, E. A., Muzzin, O., and Darst, S. A. (2002) *Science* **296,** 1285–1290
48. Vassylyev, D. G., Sekine, S., Laptenko, O., Lee, J., Vassylyeva, M. N., Borukhov, S., and Yokoyama, S. (2002) *Nature* **417,** 712–719